

 Open access • Journal Article • DOI:10.1007/S12274-014-0532-X

Two-dimensional semiconductors with possible high room temperature mobility

— [Source link](#) 

[Wenxu Zhang](#), [Zhishuo Huang](#), [Wanli Zhang](#), [Yanrong Li](#)

Published on: 03 Sep 2014 - [Nano Research](#) (Tsinghua University Press)

Topics: [Electron mobility](#), [Band gap](#) and [Phonon](#)

Related papers:

- [Generalized Gradient Approximation Made Simple](#)
- [Single-layer MoS2 transistors](#)
- [Electronics and optoelectronics of two-dimensional transition metal dichalcogenides.](#)
- [Efficient iterative schemes for ab initio total-energy calculations using a plane-wave basis set.](#)
- [Electric Field Effect in Atomically Thin Carbon Films](#)

Share this paper:    

View more about this paper here: <https://typeset.io/papers/two-dimensional-semiconductors-with-possible-high-room-cmrgd2tr89>

Two dimensional semiconductors with possible high room temperature mobility

Wenxu Zhang* and Zhishuo Huang, Wanli Zhang

*State key laboratory of electronic thin films and integrated devices,
University of Electronic Science and Technology of China, Chengdu 610054, China*

Abstract

We calculated the longitudinal acoustic phonon limited electron mobility of 14 two dimensional semiconductors with composition of MX_2 , where M (= Mo, W, Sn, Hf, Zr and Pt) is the transition metal, and X is S, Se and Te. We treated the scattering matrix by deformation potential approximation. We found that out of the 14 compounds, MoTe_2 , HfSe_2 and HfTe_2 , are promising regarding to the possible high mobility and finite band gap. The phonon limited mobility can be above $2500 \text{ cm}^2\text{V}^{-1}\text{s}^{-1}$ at room temperature.

I. INTRODUCTION

Two dimensional (2D) crystals are materials with thickness of several atomic layers and extended periodically in the other two dimensions. Examples of them are monolayer or multilayer of graphene, MoS₂, BN, MoO₃ and so on. These 2D materials have now received a lot of research interests because of its unique physical properties, such as the Dirac cone in electronic band structures in graphene. Applications of these new materials have been demonstrated. High speed radio frequency devices are fabricated which make full use of the ultrahigh electron mobility in graphene. The transition-metal dichalcogenide semiconductor MoS₂ has also attracted great interest because of its distinctive electronic, optical and catalytic properties, as well as its importance for dry lubrication. Logical devices were also fabricated based on MoS₂ 2D crystals. Field effect transistors based on 2D materials are promising because it can overcome the shorted-channel effect, which is one of the biggest obstacles of further decrease of the dimensions of semiconductors¹. Thus 2D semiconductors are attractive for semiconductor technology after silicon.

Regarding to the applications of 2D materials in logical devices of semiconductors, the present materials are not good enough. Graphene has ultrahigh mobility, but it is intrinsically metallic. It is possible to open a gap at the Dirac cone, but usually the gap is tiny, and required extra parameters, for example, external electric fields, which is not easy to fully integrate it with present semiconductor processes. Monolayer MoS₂ has a direct band gap about 1.8 eV at room temperature. Transistors fabricated on 5 nm thick MoS₂ show no short channel effects down to a channel length of ~ 100 nm without aggressive gate oxide scaling¹. But the mobility was shown to be too low for practical applications at room temperature. The mobility can be enhanced by encapsulating monolayer MoS₂ in a high- k dielectric environment². On the device level, the mobility can be further engineered by electron doping. Other factors such as electrode materials are crucial to the the measured mobility³. Thus, it is important to know the intrinsic limited mobility in order to further improve the performances of the devices. The theoretical limits of these mobility is low as calculated by Kaasbjerg⁴ and Li⁵. Phonon is one of the most important scattering sources of electron transport. Phonon limited mobility in MoS₂ was carefully investigated by Kaasbjerg *et al*^{4,6}. The contributions from acoustic and optical phonon are included and electron-phonon coupling matrices are calculated by frozen phonon methods. Electron-

phonon, as well as piezoelectric interactions, are taken into account. The calculated room temperature mobility is about $410 \text{ cm}^2\text{V}^{-1}\text{s}^{-1}$ which sets the upper bound of intrinsic mobility. And also according to the work of Yoon⁷, due to the heavier electron effective mass and a lower mobility, MoS₂ is not ideal for high-performance applications. Is it possible to find other 2D semiconductors with suitable band gap and higher mobilities? High throughput calculations based on density functional theory (DFT) has been shown to be a fast way to screen out materials with desirable properties if suitable descriptors are invented. Ciraci *et al*⁸ predicted 52 different stable MX₂ single layer compounds from 88 different combinations. Lebègue *et al*⁹ use data filtering and *ab initio* calculations and screen 92 2D compounds out of the whole ICSD database. In this work, we performed electronic calculations of the selected semiconductors with composition of MX₂, where M (= Mo W, Sn, Hf, Zr or Pt) is the transitional metal, and X is S, Se or Te. In order to fast screen out the materials with high performances, mobility limited by long wave acoustic phonon was estimated by calculating the deformation potential. We found that out of the 14 compounds, three compounds, MoTe₂, HfSe₂ and HfTe₂, are promising regarding to their mobility and band gap. The phonon limited mobility can be above $2500 \text{ cm}^2\text{V}^{-1}\text{s}^{-1}$.

II. CALCULATION DETAILS

The calculations were performed by the full-potential local-orbital code¹⁰ in the version FPLO9.00-33 with the default basis settings. All calculations were done within the scalar relativistic approximation. The local density approximation functional was chosen to be that parameterized by Perdew and Wang.¹¹ The number of k-points in the whole Brillouin zone was set to $32 \times 32 \times 5$ in order to ensure the convergency of the results. Convergency of the total energy was set to be better than 10^{-8} Hartree together with that of the electron density better than 10^{-6} in the internal unit of the codes. Supercell with vacuum layer of 30 \AA was used to model the 2D nature of the compounds within the 3D crystal cell. Within the deformation potential approximation^{12,13}, the electron mobility (Takagi model) is approximated by

$$\mu = \frac{e\hbar^3\rho V_s^2}{k_B T m_e m_d E_{el-ph}^2} = \frac{e\hbar^3 c_{11}}{k_B T m_e m_d E_{el-ph}^2} \quad (1)$$

where k_B and \hbar are the Boltzmann constant and the Planck constant, respectively. m_e is the effective mass of electron and m_d is the electron density of state mass. ρ is the

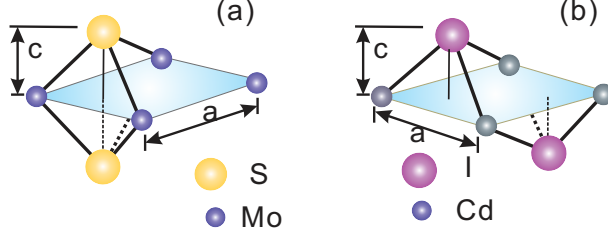


FIG. 1: Schematic illustration of the crystal structure of MoS₂ and CdI₂. The lattice parameters are a and c .

density of the material and V_s is the sound velocity in the corresponding direction. Li *et al*⁵ calculated the electrical transport of monolayer MoS₂ by the linear response method. It shows that the longitudinal phonon have the strongest interaction with electrons. Bruzzone and Fiori used this Takagi model to compute the electron mobility of hydrogenated and fluorinated graphene as well as h-BCN from first principles¹⁴ and show that graphene with a reduced degree of hydrogenation can compete with silicon technology. The sound velocity (V_s) is calculated by the supercell method, where frozen phonon mode corresponding to the longitudinal phonon with vector $\mathbf{q} = \frac{\pi}{8a}(1, 0, 0)$ was simulated. The phonon frequency (ω_k) was obtained, which is related to the sound velocity by $\omega_k = V_s q$. The elastic constants c_{11} in hexagonal crystal is related to the sound velocity by $c_{11} = \rho V_s^2$. The electron phonon coupling (E_{el-ph}) was approximated by the deformation potential. Crosschecking of the calculated parameters was done with pseudo-potential code Quantum Espresso¹⁵.

III. LONG WAVE ACOUSTIC PHONON LIMITED MOBILITY IN MX₂

Out of the ICSD database, only 16 compounds with MX₂ are semiconductors⁹. There are more layered compounds with more chemical elements. The complexity may hinder its applications. We selected 14 MX₂ compounds which crystallizes into two different crystal structures. One is MoS₂ and the other is CdI₂. The difference is that the anion hexagonal nets are A-A stacked in MoS₂, while they are A-B stacked in CdI₂ as shown in Fig.1. The phonon limited mobility for the 14 semiconductors are listed in Tab. I. The other parameters which determined the mobility according to Equ.(1) are also listed in the table. The distance between M and X are $d_{M-X} = \sqrt{(a^2/3 + c^2)}$. We plotted d_{M-X} as a function of the summation of atomic covalent radii of M and X ($r_M + r_X$) as shown in Fig.2. The data

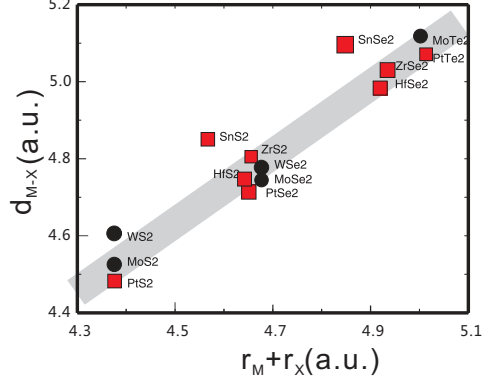


FIG. 2: Distances of M and X vs. covalent radii of the components (r_M+r_X). The shadowed area is for guiding eyes.

show a good linear proportionality. This is in accordance with the covalent bonding of the material. The sound velocity in MoS₂ is 7.93 km/s, which is the highest value among the compounds, while that of HfSe₂ with 4.72 km/s is the lowest. This leads to the relatively high elastic constant c_{11} in MoS₂ and low value in HfSe₂. Among the compounds, MoS₂, WS₂ and PtS₂ have large c_{11} 's, but their mobilities are not large. The differences of the mobility among the compounds are mostly within 50%.

The electron effective mass is almost isotropic in the compounds with MoS₂ structure, while it is quite anisotropic in the compounds with CdI₂ structure. The difference can be as large as ten folds, but the three compounds with Pt is an exception, where the effective mass is almost isotropic. The difference in the effective mass leads to anisotropic transport properties as studied in bulk materials of HfS₂.

The mobility of MoS₂ were calculated by Li⁵, where a full treatment of scattering by phonon was done. The electron phonon interaction matrices were calculated in the perturbation way. It can be seen that in the case of MoS₂, the acoustic phonon limited mobilities at 300 K obtained by the two methods are quite comparable. It is 320 cm²V⁻¹s⁻¹ if the full contributions from phonon were included, while it is 340 cm²V⁻¹s⁻¹ in our results. The sound velocity of longitudinal acoustic phonon and intra valley deformation potential extracted by Li are 6.6 km/s and 3.20 eV, comparable with our results of 7.93 km/s and 3.90 eV.

The electron phonon coupling constant and the electron effective mass in the denominator play the most important role in determining the electron mobility. The mobility and

TABLE I: Structural, mechanical and electronic parameters of the semiconductors calculated by LDA. The effective mass in the $\Gamma - K$ direction for the MoS_2 structure and $\Gamma - M$ direction for the CdI_2 structure is calculated.

MX_2	a	c	V_s	c_{11}	$m_{\Gamma-K(M)}^*$	m_{K-M}^*	E_{el-ph}	μ
	(a.u.)	(a.u.)	(km/s)	(10^{11}N/m^2)	(m_e)	(m_e)	(eV)	($\text{cm}^2/\text{V}\cdot\text{s}$)
MoS_2	5.927	2.962	7.93	6.25	0.45	0.45	3.90	340
MoSe_2	6.168	3.156	6.01	4.94	0.52	0.52	3.65	240
MoTe_2	6.618	3.411	5.04	4.45	0.53	0.57	0.92	2526
WS_2	6.047	2.992	6.67	6.52	0.24	0.26	3.92	1103
WSe_2	6.166	3.164	5.55	5.66	0.33	0.31	3.78	705
SnS_2	6.879	2.797	6.18	3.42	2.11	0.21	3.55	306
SnSe_2	7.165	2.999	4.83	2.71	2.91	0.17	2.91	447
HfS_2	6.731	2.750	5.86	4.33	3.30	0.24	1.31	1833
HfSe_2	6.944	2.978	4.72	3.37	3.10	0.18	1.08	3579
ZrS_2	6.817	2.771	7.21	4.05	1.62	0.31	1.52	1247
ZrSe_2	7.007	3.008	5.42	3.18	2.03	0.22	1.25	2316
PtS_2	6.670	2.327	6.61	7.05	0.26	0.25	3.63	1107
PtSe_2	6.978	2.464	4.73	4.26	0.21	0.19	2.86	1892
PtTe_2	7.485	2.634	4.89	4.72	0.90	0.77	1.73	367

the electron phonon coupling constant are plotted in Fig. 3 and 4. Combined with the small effective mass, MoTe_2 , HfSe_2 and ZrSe_2 show a large upper bound of acoustic limited mobility. The values are even ten times larger than the well studied MoS_2 .

IV. ELECTRONIC STRUCTURES

We have seen that these compounds have two different structures. The MoS_2 structure and CdI_2 structure which are different only by a relative shift of the anion hexagonal. This structural difference leads to different electronic structure. We show only the electronic bands of the compounds with possible high mobility. The bands of MoTe_2 are shown in Fig.5(a), while those of MoS_2 which are extensively studied in literatures are shown in

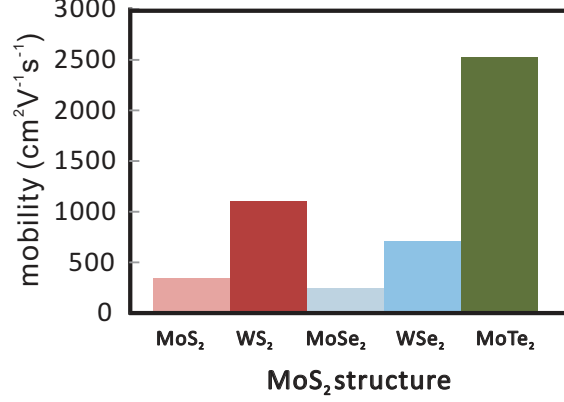


FIG. 3: Electronic mobility of compounds with MoS₂ structure.

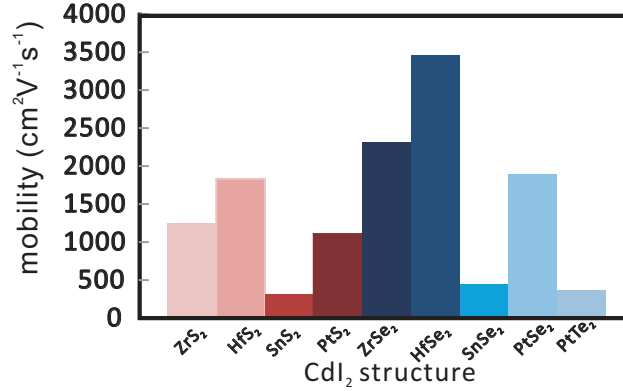


FIG. 4: Electronic mobility of compounds with CdI₂ structure.

Fig.5(b). Both of them are direct band gap semiconductors. The valence band maximum (VBM) and conduction band minimum (CBM) are located at the K -point. The direct band gaps in these compounds are 1.16 eV (MoTe₂) and 1.82 eV (MoS₂), respectively. There is a second local minimum along the $\Gamma - K$ direction. These local minima are 0.13 eV and 0.10 eV above the CBM in MoS₂ and MoTe₂ respectively. This is considered as a possible scattering states for electrons as discussed by Li⁵. It can dramatically decrease the electron mobility because of the increased scattering rate. The VBM in MoS₂ is only 0.09 eV above the local maximum at the Γ -point. However it is a quite heavy hole as indicated by the small curvature of the bands compared with that at K -point.

The bands of HfSe₂ and ZrSe₂ are different from those of MoTe₂, because of different crystal symmetry and atomic bonding. But there is a great similarity of the bands of the two compounds as shown in Fig.6. It can be seen that the dispersions around the M -point of the compounds with MoS₂ structure are quite isotropic while those with the CdI₂

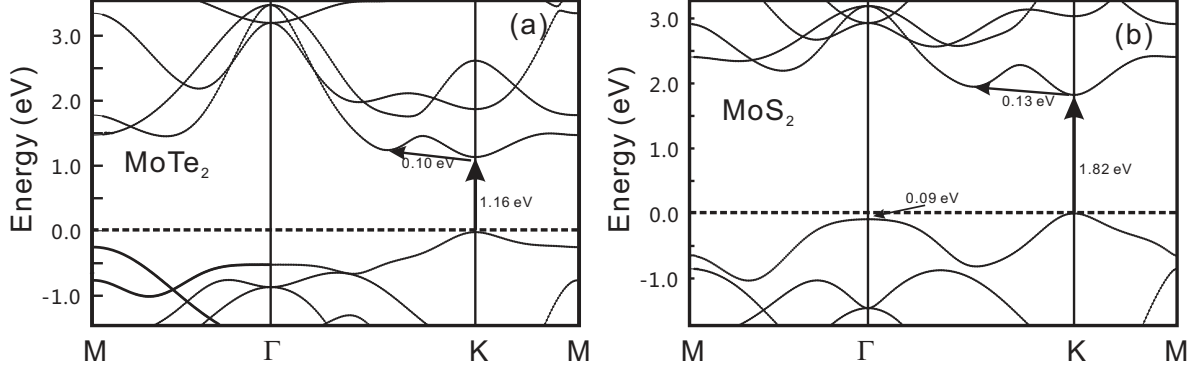


FIG. 5: Band structure of MoTe₂(a) and MoS₂(b). The arrows show the energy differences between the extremals.

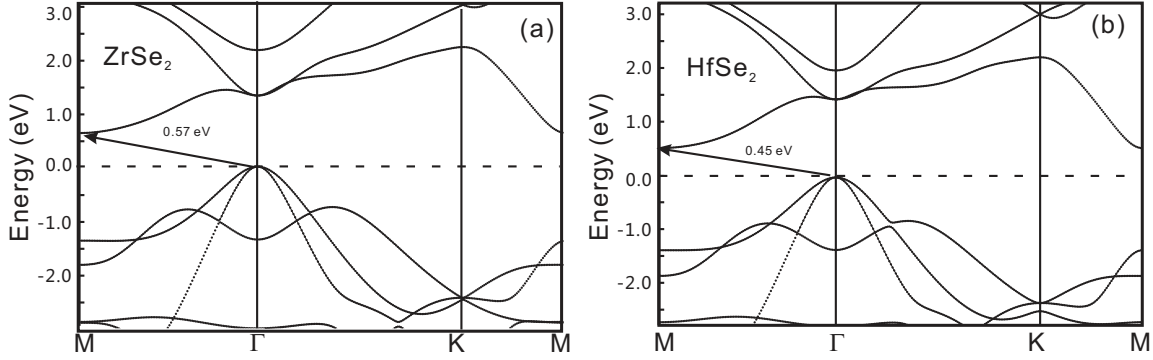


FIG. 6: Band structure of ZrSe₂(a) and HfSe₂(b). The arrows show the energy differences between the extremals.

structure are anisotropic. This leads to the different electron masses along the different directions as already shown in Table I. The effective mass in the $\Gamma - M$ direction is about ten times larger than that in the $M - K$ direction. Compounds with the MoS₂ structure are direct gap semiconductors while those with the Cd₂ structure have indirect gaps. The indirect LDA bandgap is between the Γ -point and M -point. The bandgap E_g are 0.57 eV and 0.45 eV for ZrSe₂ and HfSe₂, as shown in Figs. 6(a),6(b) respectively.

V. DISCUSSIONS

In this work, we have considered only the long wave acoustic phonon scattering. Of course, there are many other scattering mechanisms which limits the mobility. As the Matthiessen rule, i.e., $\frac{1}{\mu_{total}} = \frac{1}{\mu_{phonon}} + \frac{1}{\mu_{impurity}} + \frac{1}{\mu_{electron}} + \dots$, where the scattering sources are phonons,

impurities, electrons and so on, may hold, the mobility will be limited by any one of these mechanisms. There are uncertainties to precisely determine the contributions from each of these mechanism, both experimentally and theoretically, so that we cannot predict the mobilities precisely. However, by computing selected one of them, the upper bound of the mobility can be set. We thus can say, it is hopefully that we can find compounds with possible high mobility among the selected ones with larger upper bounds. More sophisticated calculations are needed to aim more precisely. However, these calculations are time consuming for search within the large amount of candidates.

According to our estimation, the mobility of WSe_2 may be larger than MoS_2 . Mobilities of WSe_2 and MoS_2 are extracted from the transfer character curves of field-effect transistors¹⁶. It is shown that the electron mobility in WSe_2 is about $110 \text{ cm}^2\text{V}^{-1}\text{s}^{-1}$, while that of MoS_2 is about $25 \text{ cm}^2\text{V}^{-1}\text{s}^{-1}$. These experimental results can be an example of our prediction.

VI. CONCLUSION

In this work, the electron mobility of 14 MX_2 type two dimensional semiconductors were calculated where only elastic scattering from long wave acoustic phonon was taken into account by the deformation potential approximation. We found that the mobility of the semiconductors with CdI_2 structures are generally larger than that of MoS_2 structure. However, the electronic bands are anisotropic with the CdI_2 , which means that their electronic transport properties are dependent on directions. MoTe_2 , ZrSe_2 and HfSe_2 are more promising two dimensional semiconductor than MoS_2 when considering their possible larger carrier mobilities and sizeable band gap. The acoustic phonon limited electron mobility are above $2000 \text{ cm}^2\text{V}^{-1}\text{s}^{-1}$ at room temperature.

VII. ACKNOWLEDGEMENT

Financial support from the Research Grant of Chinese Universities and International Science & Technology Cooperation Program of China (2012DFA51430) are acknowledged.

* Electronic address: xwzhang@uestc.edu.cn

- ¹ Han Liu, Adam T. Neal, and Peide D. Ye. *ACS Nano*, 6(10):8563–8569, 2012.
- ² B. Radisavljevic and A. Kis. *Nature Materials*, 12:815–820, 2013.
- ³ I. Popov, G. Seifert, and D. Tománek. *Phys. Rev. Lett.*, 108:156802, 2012.
- ⁴ K. Kaasbjerg, K.S. Thygesen, and K.W. Jacobsen. *Phys. Rev. B*, 85:115317, 2012.
- ⁵ X. Li, J.T. Mullen, Z. Jin K.M. Borysenko, M.B. Nardelli, and K.W. Kim. *Phys. Rev. B*, 87:115418, 2013.
- ⁶ K. Kaasbjerg, K.S. Thygesen, and A.P Jauho. *Phys. Rev. B*, 87:235312, 2013.
- ⁷ Youngki Yoon, Kartik Ganapathi, and Sayeef Salahuddin. *Nano Letters*, 11(9):3768–3773, 2011.
- ⁸ C. Ataca, H. Şahin, and S. Ciraci. *The Journal of Physical Chemistry C*, 116(16):8983–8999, 2012.
- ⁹ S. Lebègue, T. Björkman, M. Klintonberg, R.M. Nieminen, and O. Eriksson. *Phys. Rev. X*, 3:031002, 2013.
- ¹⁰ K. Koepernik and H. Eschrig. *Phys. Rev. B*, 59:1743, 1999.
- ¹¹ J.P. Perdew, K. Burke, and M. Ernzerhof. *Phys. Rev. Lett.*, 77:3865, 1996.
- ¹² J. Bardeen and W. Shockley. *Phys. Rev.*, 80:72–80, 1950.
- ¹³ Shin-chi Takagi, Judy L. Hoyt, Jeffrey J. Welser, and James F. Gibbons. *Journal of Applied Physics*, 80(3):1567–1577, 1996.
- ¹⁴ S. Bruzzone and G. Fiori. *Appl. Phys. Lett.*, 99:222108, 2011.
- ¹⁵ Paolo Giannozzi, Stefano Baroni, Nicola Bonini, Matteo Calandra, Roberto Car, Carlo Cavazzoni, Davide Ceresoli, Guido L Chiarotti, Matteo Cococcioni, Ismaila Dabo, Andrea Dal Corso, Stefano de Gironcoli, Stefano Fabris, Guido Fratesi, Ralph Gebauer, Uwe Gerstmann, Christos Gougoussis, Anton Kokalj, Michele Lazzeri, Layla Martin-Samos, Nicola Marzari, Francesco Mauri, Riccardo Mazzarello, Stefano Paolini, Alfredo Pasquarello, Lorenzo Paulatto, Carlo Sbraccia, Sandro Scandolo, Gabriele Sclauszero, Ari P Seitsonen, Alexander Smogunov, Paolo Umari, and Renata M Wentzcovitch. *Journal of Physics: Condensed Matter*, 21(39):395502 (19pp), 2009.
- ¹⁶ Hui Fang, Mahmut Tosun, Gyungseon Seol, Ting Chia Chang, Kuniharu Takei, Jing Guo, and Ali Javey. *Nano Letters*, 13(5):1991–1995, 2013.